Desalination 265 (2011) 153–158

Contents lists available at ScienceDirect

Desalination

journal homepage: www.elsevier.com/locate/desal

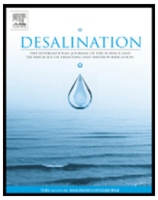

Synthesis and desalination performance of Ar^+–N^+ irradiated polysulfone based new NF membrane

Chitrakara Hegde [a], Arun M Isloor [b,*], Mahesh Padaki [b], Pikul Wanichapichart [c,d], Yu Liangdeng [d,e]

[a] Department of Chemistry, Nitte Meenakshi Institute of Technology, Yelahanka, Bangalore, India
[b] Membrane Technology Division, Chemistry Department, National Institute of Technology, Surathkal, Mangalore 575 025, India
[c] Membrane Science and Technology Research Center, Department of Physics, Prince of Songkla University, Songkhla, Thailand
[d] ThEP Center, CHE, 328 Si Ayutthaya Rd., Bangkok 10400, Thailand
[e] Fast Neutron Research Facilities, Department of Physics, Chiangmai University, Thailand

ARTICLE INFO

Article history:
Received 5 April 2010
Received in revised form 20 July 2010
Accepted 20 July 2010
Available online 18 September 2010

Keywords:
RO membrane
NF membrane
Surface modification
Filtration
Plasma treatment

ABSTRACT

In the last few years, membrane technology has gained more attention from polymer chemists throughout the globe. Nowadays, surface modification of membrane is very useful in biotechnology and food science. In the present investigation, we have synthesized polysulfone based composite nanofiltration (NF) membranes, and characterized these membranes by FT-IR, SEM and membrane performance studies. Surface plasma treatment was carried out by irradiation with argon and nitrogen beams in suitable conditions. It was observed that nitrogen beam caused surface roughness that was more severe than the Ar beam. After irradiation, water contact angle was slightly increased. For pure water permeability, flux increased linearly with the operating pressure. However, for the salt solution, the flux was decreased marginally and salt rejection increased after irradiation due to surface modification. The modification effect was characterized in terms of contact angle, AFM employed roughness measurement and dielectric property. It revealed that irradiated NF membranes showed higher salt rejection and lower flux as compared to the nonmodified membranes. Accordingly, the roughness of the membrane surface intensively affected the performance of RO membrane.

1. Introduction

The need for drinking water with good microbiological and chemical quality is clearly increasing around the world. Simultaneously, membrane processes have met a large expansion in desalting of brackish and seawater in the two last decades. In the 20th century, membrane technologies have made great progress, and commercial markets have been spreading very rapidly. Porous membranes are a major tool in water treatment. The transfer mechanism of RO membranes involves both pore flow and solution diffusion. Categorically, four types of membranes are distinguished, namely reverse osmosis (RO), nanofiltration (NF), ultrafiltration (UF) and microfiltration (MF) [1]. At present, reverse osmosis (RO) is the best possible membrane process in liquid/liquid separation. Because of vastly expanding populations, increasing water demand, and the deterioration of water resource quality and quantity, water is going to be the most precious resource in the world. Therefore, RO membranes play very crucial roles in obtaining fresh water from nonconventional water resources such as seawater and wastewater [2]. Not only in water treatment, but by tailoring appropriate [3] pore size, pore structure and pore distribution, membranes can be used for fuel cell and other filtration applications too.

According to Zhou et al. [4], in RO and NF membranes, water molecules (0.27 nm) permeate while hydrated salt ions (e.g. Na^{+1} 0.72 nm diameter) are rejected. The efficiency of the membrane can be improved by two methods, the phase inversion method and surface modification by interfacial polymerization for thin film composite membranes. The pore size of the membrane can be controlled by phase inversion techniques but getting symmetric pores is still a big challenge. Usually, composite RO and NF membranes are prepared by phase inversion technique [5]. Recently, surface modification [6] has been used to increase the efficiency of RO membranes, thin film composites [5] and charged surface membranes [7].

Recently, the transport parameters of the RO composite membranes have been tested by performing electron radiation and gamma radiation on RO composite membranes, so that these membranes can be used in the treatment of radioactive liquid effluents with an activity that involves an absorbed dose in the membrane within the studied range [8].

Cold plasma treatment to the polymers changes their properties such as biocompatibility permeability, adhesion, and hydrophilicity. The surface reactions on polymers are etching, cleaning, cross-linking,

---

* Corresponding author. Tel.: +91 824 2474000x3206; fax: +91 824 2474033.
E-mail address: isloor@yahoo.com (A.M. Isloor).

0011-9164/$ – see front matter © 2010 Elsevier B.V. All rights reserved.
doi:10.1016/j.desal.2010.07.046

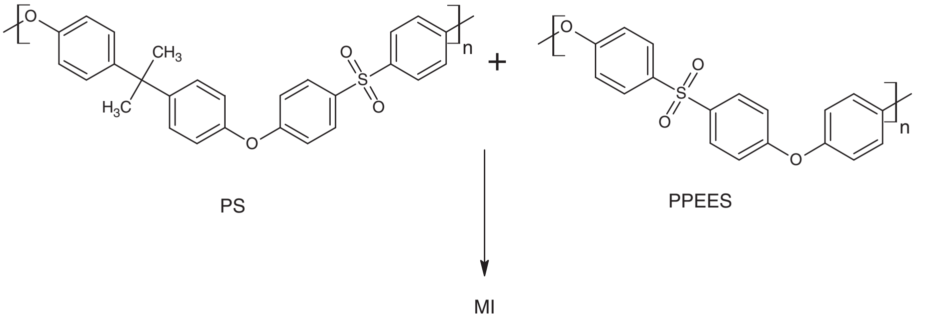

Fig. 1. Schematic representation of formation of composite membrane (M1).

grafting, addition, substitution, and formation of functional groups depending on the presence of active species in plasma [9]. Cold plasma is a mixture of electrons, ionized gas and molecular fragments of the gas. Its contents and effect on the material surface depend on the composition of the gas in the discharge, the composition of the sample treated and all the process parameters. This type of surface modification is effective for water purification [10].

A very popular technique is surface grafting—a technology that can provide polymers with a new, stable and monofunctional surface. The most versatile technique seems to be cold plasma and its applications for treatment of polymer surfaces have grown rapidly in the last decade. A great contribution to this is the fact that plasma techniques are fast, clean and environmentally friendly [11].

In the present investigation, we have synthesized polysulfone based nanofiltration (NF) membranes, and characterized these membranes by FT-IR, SEM and membrane performance studies. Surface modification was done by bombarding with argon and nitrogen under suitable conditions. The modified polymer was characterized by the contact angle, AFM and dielectric property. The desalination properties of surface-modified membranes were compared with the original membrane [12].

2. Experimental

2.1. Materials and methods

Polysulfone (PS) with a molecular weight of 35,000 Da and poly (1,4-phenylene-ether-ether sulfone) (PPEES) were obtained from Sigma-Aldrich, Co., Germany. 1-Methyl-2-pyrrolidone (NMP) and analytical grade NaCl were procured from Merck India, Ltd. These were used without any further purification.

Solutions containing 80 wt.% of PS (0.8 g) and 20 wt.% of PPEES (0.4 g) in 4.5 ml of 1-methyl-2-pyrrolidone (NMP) were prepared by mild stirring for 24 h at a constant temperature of 65 °C. The so obtained viscous solution was cast over a glass plate using K-Control coater. Further the cast membrane was kept for slow solvent evaporation and finally the membrane (M1) (Fig. 1) was separated by spraying water at the sides and stored in double distilled water [13–15].

2.2. Plasma treatment

Irradiation with N^+ and Ar^+ beams was carried out in a vacuum chamber [13]. Since the mass of Ar^+ is larger, the energy used for beam bombardment was chosen to be double of that used for N^+ beams and the two energy levels used were 30 and 60 kV, respectively. Membranes were then characterized for water contact angle (contact angle meter, model OCA 15 EC, Data Physics Company), surface roughness using atomic force microscopy (Nanosurf®, easyScan2), and dielectric constant using LCR meter (Agilent Technologies) [16].

2.3. Flux-retention measurement

Flux-retention measurements were carried out with a 3.5% sodium chloride solution (35,000 ppm) at different pressures ranging from 2 to 14 bar pressure. Pure water was prepared using Milli-Q-Plus demineralising unit and pure water permeability was measured. The flux-rejection measurements were carried out in a stirred dead-end filtration set-up containing membranes with an area of 12.5 cm^2. The stirred permeation cell was pressurized by nitrogen. The obtained data was recorded as a function of pressure by means of a computer. The concentrations were determined by conductivity measurements [17–19].

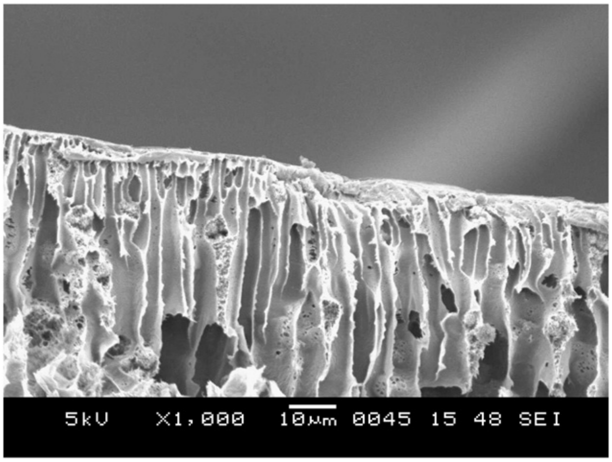

Fig. 2. Cross-section of membrane M1.

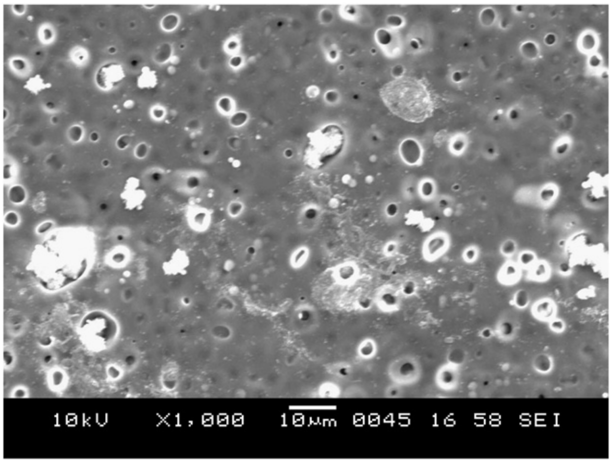

Fig. 3. Surface picture of M1.

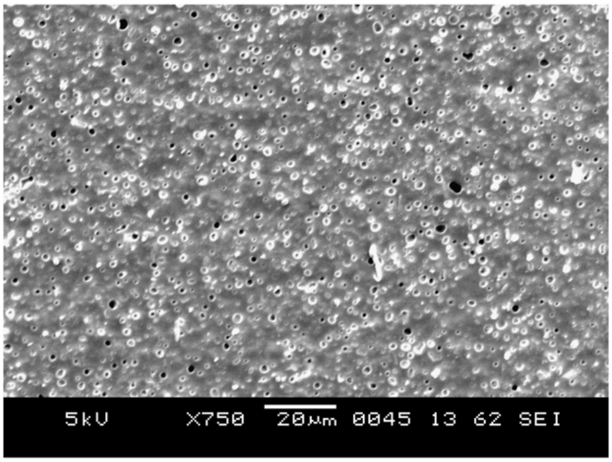

Fig. 4. Surface picture of M1.

2.4. Membrane morphology

The membrane was cryogenically fractured in liquid nitrogen and then coated with gold before the cross-section image of the membrane was observed with a Jeol JSM-6380LA, Scanning electron microscope.

3. Results and discussion

3.1. Morphology and structural characteristics

In membrane technology, the most important factors to control are membrane structure and performance (flux and rejection). These membrane performances could be monitored by adopting appropriate pore distribution, pore structure and pore size. SEM is a powerful tool to investigate the pore size of the membranes. A cross-section of the membrane was generally distinguished into three layers—the top layer, an intermediate layer, and a sublayer. All cross-sections of the membrane showed small dense pores in the top layer followed by medium pores in the intermediate layer and a thick sublayer having relatively bigger pore size with finger-like structures. Surface views of the membranes show that the surface is smooth and loosely packed with small pores under 3500× magnification of the M1 membrane (5–80 nm size).

The cross-section image of the composite membrane in Fig. 2 clearly shows that there is a thin selective layer on a finger-like “micro void” support layer suggesting the composite structure of this membrane. Meanwhile, the surface pictures (Figs. 3 and 4) give an overall view of pore size and pore distribution [12–17]. From the SEM image, it is certain that the spongy layer provides the sustained structure that could support high pressure. The porous finger-like layer allows transport in the permeated solvent.

The membrane performance mainly depends upon fabrication conditions, which apparently affect the membrane. The effect of heat treatment during evaporation is also another important factor which affects salt rejection. Previous experiments showed that [20] increasing heat treatment time increases the salt rejection. This is due to variations in the cross-linkings.

Table 1
Comparing water contact angle of M1 membrane, before (control) and after ion beam irradiation.

Ion irradiation	Fluences (ion cm^{-2})	Contact angles
Control M1	0	91.3 ± 1.8
30 kV, N$^+$ beams	1.25×10^{14}	98.7 ± 2.7
	2.50×10^{14}	101.0 ± 0.9
	5.0×10^{14}	99.9 ± 7.1
	10×10^{14}	96.4 ± 2.8
60 kV, Ar$^+$ beams	5×10^{14}	102.4 ± 2.5
	10×10^{14}	99.8 ± 4.8

Table 2
Comparing pure water flux with pressure for virgin membrane (M1) and irradiated membranes.

Pressure in bar	Flux (L/m^2 h) before irradiation	Flux (L/m^2 h) after Ar$^+$ irradiation	Flux (L/m^2 h) after N$^+$ irradiation
2	1.95	1.85	1.62
4	3.68	3.40	2.90
6	6.1	5.65	4.76
8	7.9	7.30	6.30
10	9.85	9.10	6.95
12	11.8	8.95	7.60
14	13.79	10.10	8.20

3.2. Influences from N$^+$ and Ar$^+$ beams

After M1 was irradiated with N$^+$ and Ar$^+$ beams, water contact angle was slightly increased in all cases, as shown in Table 1. It should be pointed out that the increased N$^+$ dosage from 1.25×10^{14} to 10×10^{14} ion cm^{-2} has no effect on the increased contact angle. This is also true for Ar$^+$ beams, of which the increased dosage increased the contact angle to a similar value. This result indicates that the contact angle seems to be mainly dependent on membrane materials but not on the ion energy and species. The changes in the contact angle do not relate to the membrane surface roughness. The results also confirm the lower hydrophilic (polysulfone based) nature of the membrane material. This is well-understood by average pure water permeability of membrane (Table 2). Table 1 shows a comparison of contact angle with ion beam irradiation [21].

On the surface morphology, AFM pictures show less roughness on the membrane without irradiation, that is even well understood by average flux-rejection rates shown by membrane. On the other hand, the N beam causes surface roughness that is more severe than the Ar beam (Figs. 5–7). This might be because N ions are smaller than Ar ions, and hence, with larger kinetic energy, they could penetrate deeper into the membrane. These morphologies further proved the results of unevenness obtained from SEM photographs [12–18,21].

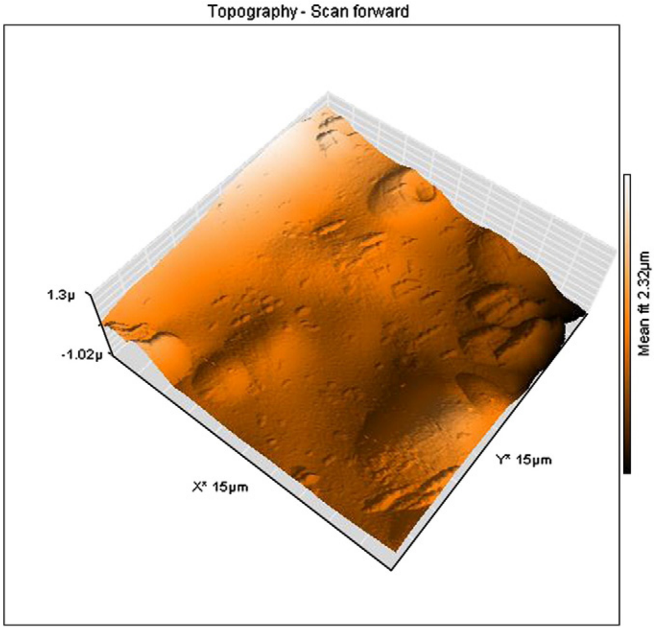

Fig. 5. AFM picture of M1 without irradiation.

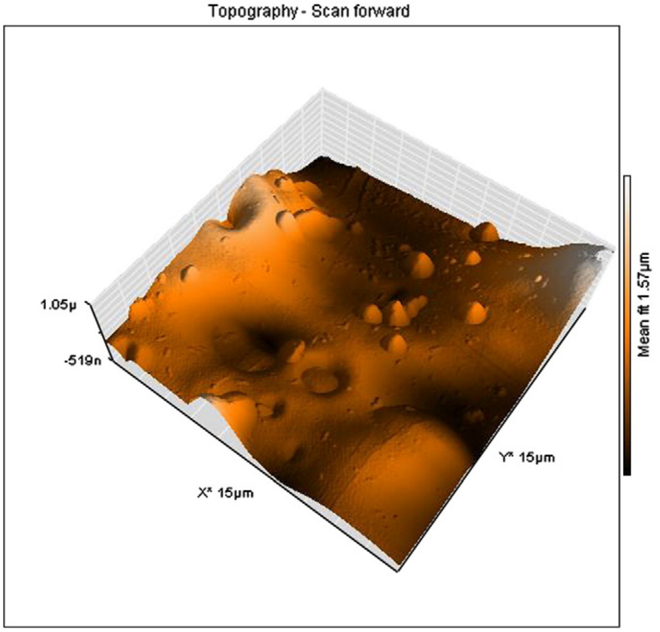

Fig. 6. AFM picture of M1 after irradiation with 30 kV N^+ beam.

The value of dielectric strength for a specimen is also influenced by its temperature and ambient humidity, by any voids or foreign materials in the specimen, and by the conditions of the test, so that it is often difficult to compare data from different sources. For membrane porosity aspect, the N^+-treated membrane in Fig. 8 shows relatively larger dielectric property, indicating greater void volume. This agrees well with the finding of more roughness due to ion penetration in the membrane.

3.3. Pure water permeability

Pure water permeability was obtained by measuring the flux for pure water against operating pressure. As shown in Fig. 9 and Table 2, the flux increases linearly with the operating pressure. This linear behavior is described by a slope, close to pure water permeability, according to the Spiegler–Kedem model [22]. For this purpose, an in-house, self-assembled instrument was used (Fig. 10). A circular membrane sample with diameter of 60 mm was placed in the test cell, the active surface facing towards the incoming feed water. The flux was measured by direct measurement of the permeate flow in terms of liters per meter square per hour (L/m^2 h). Membranes were dipped in distilled water for 24 h prior to the water permeability test for swelling, which enlarges the pore size. Nitrogen gas was used to build the pressure for operating the instrument. Pressure was serially increased at an increment of 2 bars at a time.

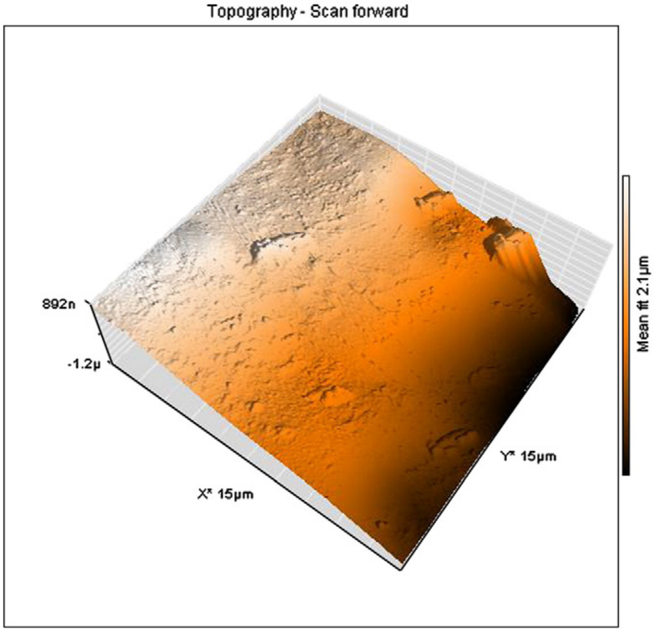

Fig. 7. AFM picture of M1 after irradiation with 60 kV Ar^+ beam.

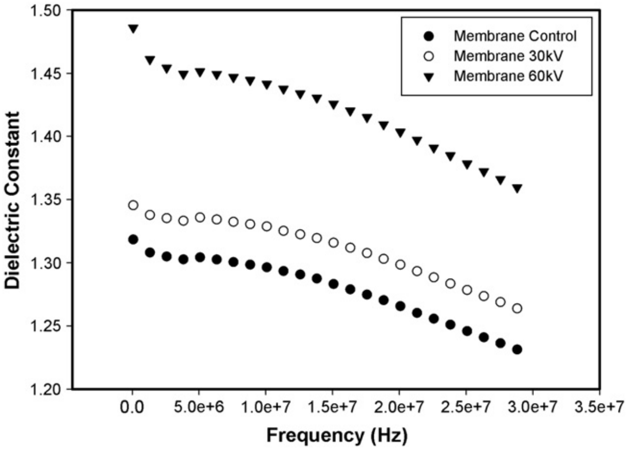

Fig. 8. Comparing dielectric property of 30 kV N^+ and 60 kV Ar^+-treated membranes with the control M1.

3.4. Effect of the kind of salt solution on membrane performance

The percentage of salt rejection was determined by comparing the conductivity of feed and permeate solutions, these samples were analyzed for their salt concentrations by conductivity measurement using the results from the present retention:

$$R_i(\%) = \left(1 - C_{ip} / C_{if}\right)$$

where C_{ip} is the salt concentration in the permeate and C_{if} is the concentration in the feed [23].

The rejection and flux for 3.5% NaCl [20] (Figs. 11 and 12; Table 3) show the predictable characteristic for the smooth surface of membrane as shown by AFM image (Fig. 6). It is worth mentioning that virgin membrane gives an average 9.7 L/m^2 h flux at 12 bar pressure. However, the flux was decreased marginally and salt

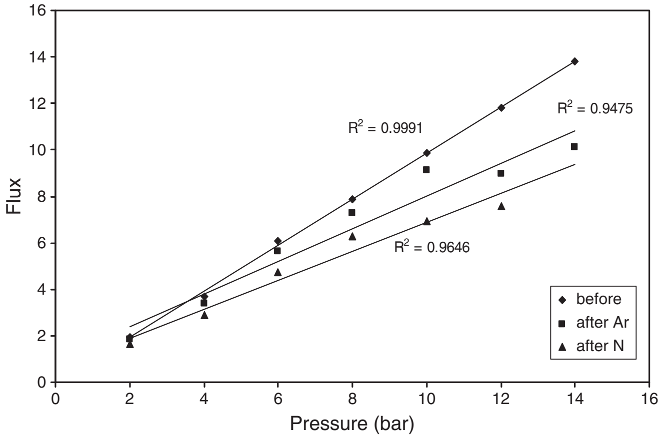

Fig. 9. Comparison curve of the flux for pure water against operating pressure.

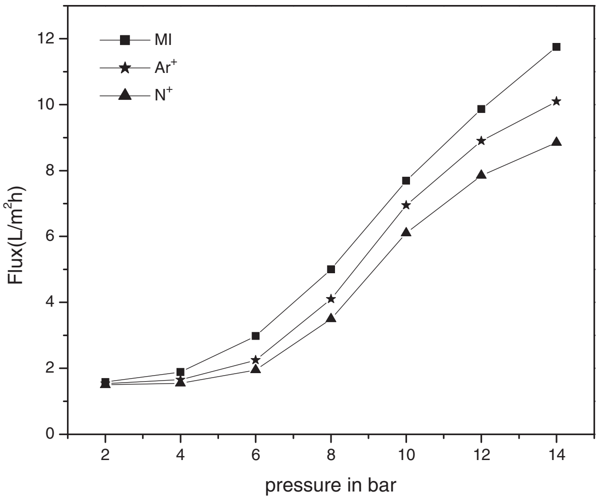

Fig. 10. Schematic picture of salinity test instrument.

rejection increased after irradiation due to the surface modification, which was clearly shown in the AFM picture. Considering the salt flux and rejection in Fig. 11, the untreated membrane shows larger flux when the applied pressure is increased. With the percentage of rejection shown, the untreated membrane is classified as nanofiltration. Irradiation of membrane surface with argon and nitrogen has blocked the larger pore sizes on the surface, thereby increasing salt rejection. As N ions are smaller than Ar, N ions have penetrated deeply in the pores than Ar ions, resulting in better salt rejection as compared to the Ar-treated membranes.

4. Conclusions

We have prepared new NF polymer composite membranes comprising of PS and PPEES by DIPS method. It was characterized by studying membrane morphologies, IR, water permeability and salt rejection. Further the membrane was irradiated by N and Ar, which resulted in a decrease of the pore size of the membrane, thereby resulting in increased salt rejection. Contact angle measurement after irradiation indicates that the contact angle is mainly dependent on membrane materials but not on the ion energy and species. The changes in the contact angle do not relate to the membrane surface roughness. It also confirms the lower hydrophilic (polysulfone based) nature of the membrane material.

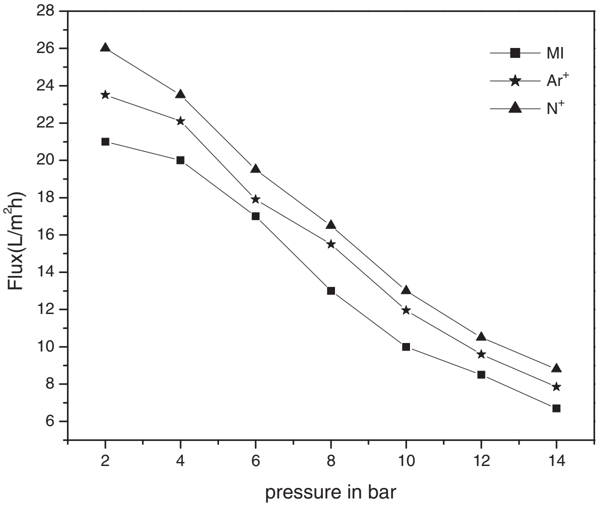

Fig. 11. Comparison of the salt flux versus pressure.

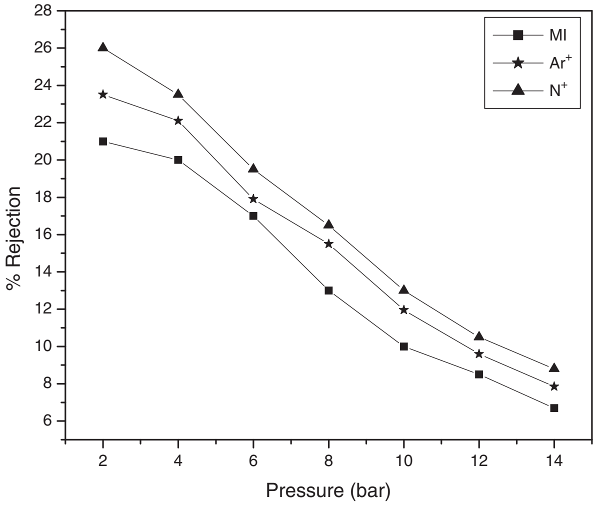

Fig. 12. Comparison of % rejection of salt versus pressure.

Table 3
Comparing salt flux-rejection rate with pressure for virgin membrane (M1) irradiated membranes using 3.5% NaCl solution.

Pressure in bar	Flux (L/m^2 h)	% rejection before irradiation	% rejection after Ar$^+$ irradiation	% rejection after N$^+$ irradiation
2	1.58	21.0	23.5	26.0
4	1.89	20.0	22.10	23.5
6	2.98	17.0	17.90	19.5
8	5.00	13.0	15.50	16.5
10	7.69	10.0	11.95	13.0
12	9.86	8.5	9.60	10.5
14	11.75	6.7	7.85	8.8

The relationship between the morphology and structure of the top surface of membranes along with their performance has been studied by using SEM, AFM and based on irradiation effect. The surface roughness of the NF membrane affects the performance of the membrane. Accordingly, in the future, further investigation on the top surface of membranes will be needed for the effects of the surface structure on the NF and RO performances.

Acknowledgements

AMI is thankful to the Board of Research in Nuclear Sciences, Government of India for “Young Scientist” award. AMI is also thankful to Prof. Sandeep Sancheti, Director, National Institute of Technology-Karnataka, India for providing research facilities and encouragement. CH is thankful to the Director, NMIT, Bangalore for financial help.

References

[1] M. Mulder, Basic Principles of Membrane Technology, Kluwer Academic Publishers, 1991.

[2] Mark Wilf, The Guide Book of Membrane Technology for Waste Water Reclamation, Balaban Desalination Publications, 2007.

[3] L.P. Raman, M. Cheryan, N. Rajagopalan, Bench-scale membrane degumming of crude vegetable oil: process optimization, Journal of American Oil Chemists Society 73 (1996) 219–224.

[4] M.J. Zhou, P.R. Nemade, X.Y. Lu, X.H. zeng, E.S. Hatakeyama, R.D. Nobel, D.L. Gen, New type of membrane material for water desalination based on cross-linked bicontinuous cubic lyotropic liquid crystal assembly, Journal of American Chemical Society 129 (2007) 9574.

[5] Zhaoxia Hu, Yan Yin, Ken-ichi Okamoto, Yukari Moriyama, Atsushi Morikawa, Synthesis and characterization of sulfonated polyimide derived from 2,2-bis(4-sulfonyl)-4,4-oxydianiline as polymer electrolyte membranes for fuel cell applications, Journal of Membrane Science 329 (2009) 146–152.

[6] Pikul Wanichapichart, Liangdeng Yu, Chitosan membrane filtering characteristics modification by N-ion beams, Surface and Coatings Technology 201 (19-20) (2007) 8165–8169.

[7] Ming-Huang Chen, Tze-Chiang chaio, Tsai-wie tseng, Preparation of sulfonated polysulfone/polysulfone and aminated polysulfone/polysulfone blend membranes, Journal of Applied Polymer Science 61 (1996) 1205–1209.

[8] P. Wanichapichart, R. Sungkum, W. Taweepreda, M. Nisoa, Characteristics of chitosan membranes modified by argon plasmas, Surface & Coating Technology 203 (2009) 2531–2535.

[9] J.M. Arnal, M. Sanchoa, G. Verdti, J.M. Campayob, J.I. Villaescusa, Treatment of ^{137}Cs liquid wastes by reverse osmosis Part I. Preliminary tests, Desalination 154 (2003) 27–33.

[10] J. Chen, J. Li, Z.P. Zhao, D. Wang, C.X. Chen, Nanofiltration membrane prepared from polyacrylonitrile ultrafiltration membrane by low temperature plasma: 5. Grafting of styrene in vapor phase and its application, Surface & Coating Technology 201 (2007) 6789–6792.

[11] Aleksander Ciszewski, Irena Gancarz, Jerzy Kunicki, Marek Bryjak, Plasma-modified polypropylene membranes as separators in high power alkaline batteries, Surface & Coating Technology 201 (2006) 3676–3684.

[12] Yao Yongyi, G. Shiwei, Z. Yunxiang, Surface properties of reverse osmosis membrane, Journal of Applied Polymer science 105 (3) (2007) 1261–1266.

[13] C. Stropnik, V. Kaiser, Polymeric membranes preparation by wet phase separation: mechanisms and elementary processes, Desalination 145 (2002) 1–3.

[14] H. Matsuyama, H. Okafuji, T. Maki, Membrane formation via thermally induced phase separation in polypropylene/polybutene/diluent system, Journal of Applied Polymer science 84 (2002) 1701–1708.

[15] J.-F. Blanco, J. Sublet, Q. Nguyen, P. Schaetzel, Formation and morphology studies of different polysulfones-based membranes made by wet phase inversion process, Journal of Membrane Science 283 (2006) 27–33.

[16] P. Wanichapichart, L.D. Yu, Chitosan membrane filtering characteristics modification by N-ion beams, Surface & Coating Technology 201 (2007) 8165–8169.

[17] C. Hegde, M. Padaki, A.M. Isloor, Synthesis, characterization and impedance study of some novel nanofiltration membranes, Iraqi Journal of Polymers 13 (2) (2009) 1–12.

[18] C. Hegde, M. Padaki, A.M. Isloor, Synthesis, characterization and proton conductivity study of some novel reverse osmosis membranes, Iraqi Journal of Polymers 13 (2) (2009) 59.

[19] L. Li, S. Zhang, X. Zhang, Preparation and characterization of poly(piperazineamide) composite nanofiltration membrane by interfacial polymerization of 3,3′, 5,5′-biphenyl tetraacyl chloride and piperazine, Journal of Membrane Science 335 (2009) 133–139.

[20] S. Jian, S.X. Ming, Crosslinked PVA-PS thin-film composite membrane for reverse osmosis, Desalination 62 (1987) 395–403.

[21] P. Wanichapichart, W. Taweepreeda, P. Choomgan, L.D. Yu, Argon and nitrogen beams influencing membrane permeate fluxes and microbial growth, Radiation Physics and Chemistry 79 (3) (2010) 214–218.

[22] Y.Z. Xu, R.E. Lebrun, Comparison of nanofiltration properties of two membranes using electrolyte and nonelectrolyte, Desalination 122 (1999) 95–106.

[23] Lei Li, Suobo Zhang, Xiaosa Zhang, Preparation and characterization of poly (piperazineamide) composite nanofiltration membrane by interfacial polymerization of 3, 3′, 5, 5′-biphenyl tetraacyl chloride and piperazine, Journal of Membrane Science 335 (2009) 133–139.